

# Research on Image Classification Model of Probability Fusion Spectrum-Spatial Characteristics Based on Support Vector Machine

**Zheng Zhang**

*Geomatics  
Xi'an University of Science and Technology  
Xi'an, 710054, China*

*bestonezheng@hotmail.com*

**Xiaobing Huang**

*Geomatics  
Xi'an University of Science and Technology  
Xi'an, 710054, China*

*happyxiaobing@hotmail.com*

**Hui Li**

*Aerial remote sensing department  
The Third Surveying and Mapping Institute of GuiZhou Province  
Guiyang, 550004, China*

*free.h\_li@hotmail.com*

---

## Abstract

For insufficient information of imaging spectrum with high spatial resolution, detailed imaging information, reduction of mixed pixels, increase of pure pixels and problems of image characteristic extraction and model classification produced from this, we provide a classifier model of a united spectrum-spatial multi-characteristic based on SVM, and use this model to finish the image classification. The model completely uses the multi-characteristic information, and overcomes the over-fitting problems produced by accumulating high-dimensional characteristics. The model includes three classifications of spectrum-spatial characteristics, namely spectral characteristics-spectral characteristic of multi-scale morphology, spectral characteristics-physical characteristics of underlying surfaces of multi-scale morphology and spectral characteristics-features spatial extension characteristics of multi-scale morphology. Firstly the three classifications of spectrum-spatial characteristics are classified through SVM, then carries out the probability fusion for the classification results based on the pixels to obtain the final image classification results. This article respectively uses WorldView-2 image and ROSIS image to experiment, and the results show that the model has better classification effect compared with VS-SVM algorithm.

**Keywords:** High Spatial Solution, Spectral - Space Characteristics, Multi-Scale Morphological Sequence, SVM.

---

## 1. INTRODUCTION

In recent years, with the continuous improvement of high spatial resolution of images, applications of image spatial characteristics in classification are promoted. For the classification of urban hyperspectral data with high spatial resolution, Benediktsson provides extended morphology sequence (EMP), which is to adopt the images of which principal components of the hyperspectral images are changed as the basic images for creating morphological sequences, and then apply the principal components of the spectrum and their EMP to a neural network classifier[3]. Because original methods do not completely consider the spectral information in the data, Fauvel changes those methods by combining the hyperspectral information with EMP to form feature vectors[4]. Huang and Zhang carries out comparative study on space approach for urban surveying and mapping by using the hyperspectral images with high

spatial resolution of Pavia in the north of Italy, extracts and classifies the features by using different spectrum-spatial characteristics, including morphological sequences (MPs), gray level co-occurrence matrix (GLCM), pixel shape index (PSI), feature-oriented classification method based on fractal network and multi-scale mean-shift algorithm; the results show that precision of pure spectral classification can be effectively improved by combining the spectrum-spatial characteristics[1][5][9].

In methods for classifying and processing the high-resolution data by combining various spatial information, the method which uses the vector superposition of each characteristic and classifies through the support vector machine has better result, but it also has following shortcomings: firstly, during the process for forming the spatial characteristics, different parameters, such as sizes, scales and directions, are needed to be set, which may form a high-dimensional characteristic space, so that the calculation complexity is increased; secondly, with the continuous increase of characteristic space, when the characteristic space dominates all the characteristic spaces, the spectral characteristics are submerged to some extent, which causes the identification error, so in order to improve the classification precision by using the spectrum-spatial characteristics and overcome the shortcomings of VS-SVM classification, we provide the image classification model of probability fusion spectrum-spatial characteristics of SVM, and apply the model to the high-resolution image classification. The model completely uses the spectrum-spatial characteristics and perfectly prevents the over-fitting problems produced by accumulating high-dimensional characteristics.

## 2. RELATED WORK

In the images with high spatial resolution, detail ground information can be completely exhibited; the inner parts of the same classifications of the features have variability, even the homogeneous areas have obvious spectrum differences, so that the interclass variance enlarges, and the separability of spectrum areas are reduced. When processing the images, we not only reduce the inner spectrum changes of the homogeneous areas, but also protect its edge and detail information, namely needing to consider the multi-scale characteristics of the features.

This article adopts the multi-scale morphological sequence which can open and close creation hybrid operation to process the spectral information. The model has three classifications of the spectrum-spatial characteristics, namely spectral characteristics-spectral characteristic of multi-scale morphology, spectral characteristics-physical characteristics of underlying surfaces of multi-scale morphology and spectral characteristics-features spatial extension characteristics of multi-scale morphology. The methods presented in this paper firstly respectively classifies the three classifications of the spectrum-spatial characteristics of the model by using the SVM classifier, and then carries out the probability fusion for the classification results based on the pixels to obtain the final image classification results.

## 3. OVERVIEW OF THE METHODS

### 3.1 Difference Multi-scale Morphological Sequence Based on CFO Operator

The bright details which are smaller than the structural bodies in the images can be smoothed and the stability of the overall characteristics can be maintained by opening the recreation function of morphology, and the dark details which are smaller than the structural bodies in the images can be smoothed and the stability of the overall characteristics can be maintained by closing the recreation function of morphology, therefore this article uses the multi-scale morphological characteristics of the morphological operators opening by reconstruction followed by closing by reconstruction (CFO) to calculate. The features of which spectrums in images are similar are easy to mix, such as the roads and the buildings with low illumination, but anisotropy and isotropy exist among the features, such that the roads have anisotropy but the buildings have isotropy, so that this article adopts the linear structural element (SE), sets as  $SE = strel('line', d, s)$ , wherein  $d$  and  $s$  respectively represent the direction and size of SE. So the CFO operators definition is as follows:

$$CFO^g(d, s) = \gamma_R^g(\phi_R^g(d, s)) \tag{1}$$

The white-hat conversion can extract the bright structures and remove the dark structures in the images, so that the areas which are smaller than the defined structural elements and brighter than the adjacent areas around can be obtained by subtracting the two images. So the White-hat conversion of CFO operators definition is as follows:

$$W - TH_{CFO}(d, s) = \phi_R^g(d, s) - CFO^g(d, s) \tag{2}$$

$\phi_R^g(d, s)$  uses the images obtained by closing the recreation for image  $g$  through SE, and  $CFO^g(d, s)$  uses the images obtained by opening the recreation for image  $\phi_R^g(d, s)$  through SE.

We do not confirm the specific sizes of the targets of interest in advance, and some specific targets are shown as multi-scale morphology in the images, so that, this article adopts the multi-scale Morphological sequence method proposed by Benediktsson[12], establishes Multi-scale morphological sequences based on CFO operator, can be known as the generalization of the characteristics on different scales, which is defined as follows:

$$\begin{cases} MP_{W-TH_{CFO}}(d, s) = W - TH_{CFO}(d, s) \\ MP_{W-TH_{CFO}}(d, o) = g \end{cases} \tag{3}$$

Combined with multi-scale morphological difference principle, we establish difference multi-scale morphological sequence based on CFO operator, which is defined as follows:

$$\begin{aligned} DMP_{W-TH_{CFO}}(d, s) = \\ \left| MP_{W-TH_{CFO}}(d, s + \Delta s) - MP_{W-TH_{CFO}}(d, s) \right| \end{aligned} \tag{4}$$

wherein  $\Delta s$  is the distances of the morphological sequences,  $s \in (s_{min}, s_{max})$ .

### 3.2 Spectral Characteristics-spectral Characteristic of Multi-scale Morphology

The spectral characteristics of the images are the basis of the image classification, but the classification results cannot achieve the satisfying effect if the images are classified by directly according to spectral characteristics, so that this article adds the spatial characteristics based on the spectral characteristics, namely multi-scale morphological operations are carried out for the spectral characteristics, recorded as SDspe, and then use the SVM classifier to classify the images. The is defined as follows:

$$\begin{aligned} DMP_{W-TH_{CFO}}^{spec}(d, S) = \\ \{ DMP_{W-TH_{CFO}}^{spec}(d_1, S_1), DMP_{W-TH_{CFO}}^{spec}(d_2, S_2), \dots, DMP_{W-TH_{CFO}}^{spec}(d_n, S_n) \} \end{aligned} \tag{5}$$

wherein  $(d, S)$  expresses the different scales of the Linear SE sequences.

### 3.3 Spectral Characteristics-features Spatial Extension Characteristics of Multi-scale Morphology

In remote-sensing images, the similarity level of the pixels of the same feature is high on the spectral characteristic, so it provides the base for extracting the pixels of the same feature. We

can use this characteristic of the features to extract the spectral-spatial extension characteristics of the features, then carry out the morphological operations for the obtained extension characteristics, and then use the SVM classifier to classify the images.

The spatial extension characteristics of the features in the images can be expressed as extension of the pixels, namely the spatial extension characteristics have succession of the pixels of which attributes are similar in the special direction. Therefore this article creates a similarity function  $\text{sim}(t, \theta, W)$  of the pixels, wherein  $t$  is responsible for the threshold values of the similarity of the pixels,  $\theta$  is responsible for the extension direction, and  $W$  is responsible for the size of the window. This article evaluates the similarity of the adjacent pixels by using the spectral angle method; for the vectors  $x$  and  $y$  of the two spectrums, the similarity level of the spectrum is determined according to the size of the included angle. If the included angle is smaller, the two spectrums are more similar. The calculation method of the spectral angle is as follows:

$$\cos(x, y) = \frac{x^T y}{\|x\| \|y\|} = \frac{x^T y}{[(x^T x)(y^T y)]^{1/2}} \quad (6)$$

This article defines the four extension directions of the centre pixel which extend to outside  $\theta$ :  $0^\circ$ ,  $45^\circ$ ,  $90^\circ$  and  $135^\circ$  shown in Figure1, and the direction of the arrow is the main direction of the extension direction. Take  $\theta=0$  for example: the size of the window in the figure is set as  $w \times w$ , the pixel  $o(i, j)$  is set as the centre pixel and its initial extension value is  $1=0$ , when the spectral angle between the pixel  $o(i, j)$  and the adjacent pixel  $o(i, j+1)$  in the main direction is not larger than some per-set threshold value  $t$ , the spectral properties of the two pixels are similar, then the extension value adds 1, and then  $o(i, j+1)$  is adopted as the new starting point to continuously solve the extension; or the similarity of the pixels  $o(i-1, j+1)$ ,  $o(i+1, j+1)$  and  $o(i, j)$  is respectively calculated, if the spectral angle between one of the points and the starting point is not larger than some pre-set threshold value, this point is adopted as the starting point to continuously calculate until to reach the border of the window; or the calculation in this direction is ended; later the calculation is repeated in the opposite direction of  $0^\circ$  to obtain the extension value  $1-$ , later the extension value  $1$  on the direction  $0^\circ$  and the value  $1-$  on the opposite direction are added, and the result is adopted as the extension characteristic, for example, the red line in Figure 2 is the extension example of  $\theta=0^\circ$ , for the similar directions, the extension values on the directions  $45^\circ$ ,  $90^\circ$  and  $135^\circ$  can be calculated. If the extension values on the four directions  $0^\circ, 45^\circ, 90^\circ$  and  $135^\circ$  are recorded as  $\{10, 145, 190, 1135\}$ , the the formulas to calculate of extension characteristic are such as Formula (7) - Formula(9).

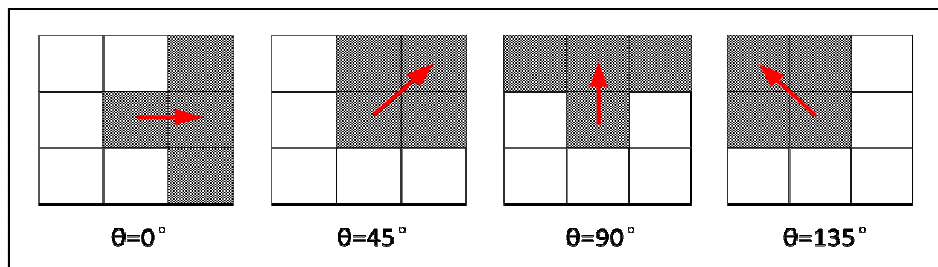


FIGURE 1: Extension of Four Directions.



underlying surfaces of multi-scale morphology(Spectral<sub>NMF</sub> -  $\text{Fraction} \text{DMP}_{W-TH_{CFO}}(d, s)$ ), record as  $\text{SD}_{\text{Fra}}$ , and classifies the support vector machines. The  $\text{Fraction} \text{DMP}_{W-TH_{CFO}}(d, s)$  is defined as:

$$\begin{aligned} \text{Fraction} \text{DMP}_{W-TH_{CFO}}(d, S) = \\ \{ \text{Fraction} \text{DMP}_{W-TH_{CFO}}(d_1, S_1), \text{Fraction} \text{DMP}_{W-TH_{CFO}}(d_2, S_2), \dots, \text{Fraction} \text{DMP}_{W-TH_{CFO}}(d_n, S_n) \} \end{aligned} \quad (11)$$

### 3.5 Probability Fusion Based on Pixels

The output results of the three support vector machine classifiers are integrated, and the final classification result shall be confirmed after passing through the maximum posterior probability, which calculation formula is as followed:

$$C(x) = \arg \max_{k=\{1, \dots, K\}} \left\{ \frac{1}{F} \sum_{f=1}^F S_f(x) \cdot p_f^k(x) \right\} \quad (12)$$

F is responsible for the sum of the spectrum-spatial characteristics,  $p_f^k(x)$  is responsible for the probability value of the pixel x in the probability output result of the SVM classification category k corresponded to the spectrum-spatial characteristic f,  $S_f(x)$  is responsible for the category certainty of the pixel x of the SVM classification corresponded to the spectrum-spatial characteristic f,  $S_f(x)$  is called the weight of the probability value  $p_f^k(x)$ , purpose for applying  $S_f(x)$  is to reduce the influence of the classification results caused by the uncertain information and increase the weight of the reliable information.

## 4. EXPERIMENTS & RESULTS

We respectively apply the model, which is proposed in this paper namely P-fusion-SVM, to the experiments of ROSIS images and WorldView-2 images. Compare the overall classification accuracy and Kappa coefficient of different classification methods, such as classification results for simply considering the spectral characteristics and each result of three classification methods which mentioned in this paper and so on, to verify the feasibility of the Classification model proposed in this paper.

### 4.1 ROSIS Image Experiment

We test the images of Pavia University's School of Management shot by ROSIS aerial optical sensor on July 8, 2002. Figure3 shows the data of the shot experimental area of Pavia University: (a) the RGB color images of the area; (b) the multispectral images of which the number of the wave bands is 3 after NMF conversion; (c) ground reference data after locally surveying and mapping. The images and the ground reference data are provided by professor Gamba of Pavia University. The number of the training samples and the test samples of the images of Pavia University refers to Table 1.

For the hyperspectral images with high resolution, we usually reduce their dimensions, and then extract the characteristic of the images. The usual dimension method is to converse the principal analysis method PCA and the non-negative matrix factorization NMF, and reduce three spectral bands.

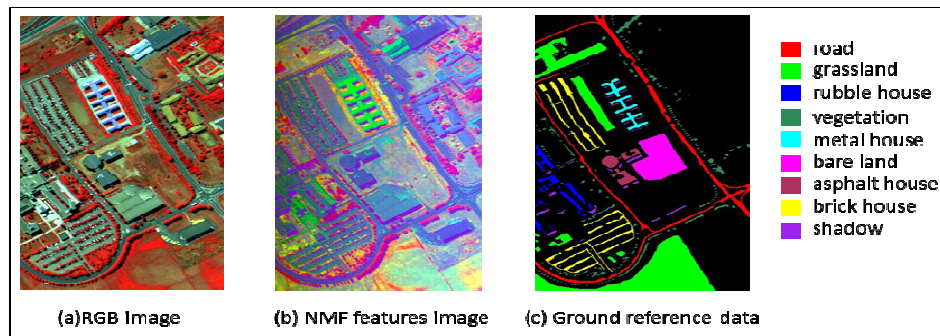


**FIGURE 3:** Data of Pavia University.

Categories	Training Samples	Test Samples
Road	530	6206
Grassland	507	16123
Rubble house	288	1880
Vegetation	251	2933
Metal house	343	1345
Bare land	367	5029
Asphalt house	221	1330
Brick house	410	3682
Shadow	254	947
Total samples	3171	39475

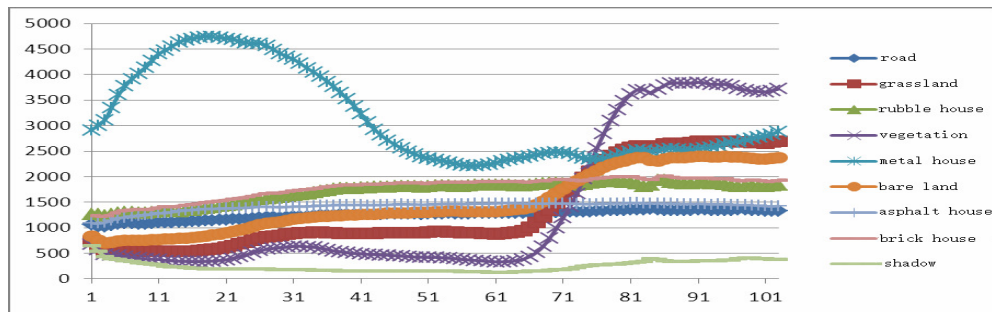
**TABLE 1:** Training Samples and Test Samples of the Images of Pavia University.

Classification Categories	Hyperspectral	NMF	PCA
	103-D	3-D	3-D
Road	80.86	81.41	76.86
Grassland	87.82	85.70	73.39
Rubble house	61.10	61.43	78.40
Vegetation	62.60	92.09	89.94
Metal house	99.04	98.88	99.78
Bare land	70.18	55.18	83.10
Asphalt house	47.73	40.23	65.49
Brick house	80.17	78.33	73.85
Shadow	99.68	99.89	99.26
OA	79.12	78.36	72.93
Kappa	73.34	72.98	66.06

**TABLE 2:** Feature Classification Precision Table Based on Different Spectral Data.

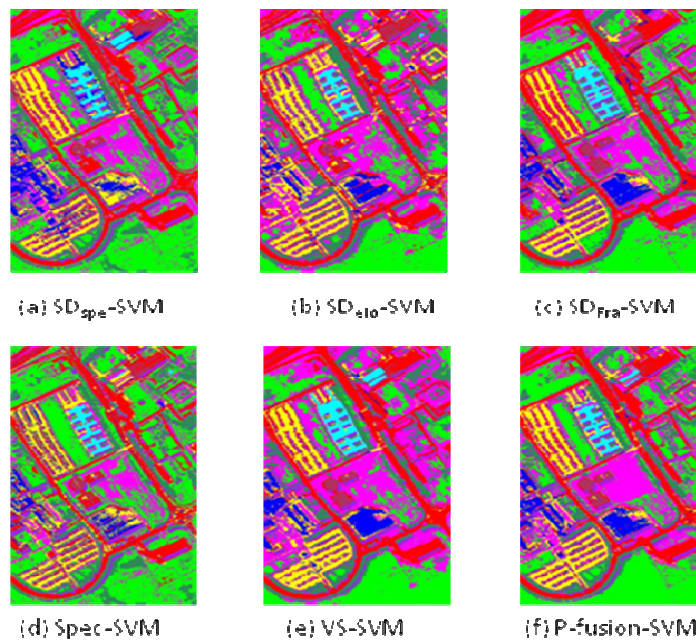
Table 2 is a feature classification precision table based on different spectral data, the spectral data includes the 103-dimensional hyperspectral data, the spectral data of which number of the wave bands is 3 after PCA conversion, and the spectral data of which number of the wave bands is 3 after NMF conversion. From the Table, the classification precision of NMF (OA=78.36%) is close to the classification precision of the 103-dimensional hyperspectral data (OA=79.12%), which is higher than the classification precision of PCA (OA=72.93%), so that NMF is rational and feasible to be adopted as the spectral characteristics of the experimental area.

Figure 4 shows the spectral curves of various features in the images of Pavia University in the hyperspectral data, each spectral curve is responsible for a classification of the special features, the spectral values of each classification of the features are the mean value of the spectral reflectance of all the samples of the features. From the Figure, the metal houses have high spectral reflectance within the whole wave band, but the reflectance of the shadow is low within the whole wave band, so that the two classifications of the features are easy to distinguish; the spectral curves of the asphalt houses, the roads, the brick houses, the rubble houses and the bare land are very similar, so we are difficult to simply distinguish them according to the spectral characteristics.



**FIGURE 4:** Spectral Curves of Various Features in the Images of Pavia University.

For this experiment, the specific parameters are set as follows: the number of the clusters of the spatial extension characteristics of the features  $K=20$ , the size of the window  $17 \times 17$ . The structural elements of the multi-scale morphological characteristics of the spatial extension characteristics of the features and the physical characteristics of the multi-scale morphological characteristics of the underlying surfaces of the ground, set the sizes as  $s=\{2\ 4\ 6\ 8\ 10\}$ , and the directions as  $d=\{45^\circ, 90^\circ, 135^\circ, 180^\circ\}$ .



**FIGURE 5:** The Results of the University of Pavia Image Classification.



In Figure 5, the classification results of the features by using different methods include: (a) the  $SD_{spe}$ -SVM classification results; (b) the  $SD_{elo}$ -SVM classification results ;(c) the  $SD_{Fra}$ -SVM classification results; (d) the SVM classification results for simply considering the spectral characteristics; (e) the VS-SVM classification results for overlaying the three classifications of the spatial characteristics and the spectral characteristics; (f) the P-fusion-SVM classification results of the feature classification model for using the probability fusion spectrum-spatial characteristics of the support vector machines. For verifying the accuracy of the model, we evaluate the precisions of the classification results by using six methods, and the evaluation results refer to Table 3.

Methods	$SD_{spe}$ -SVM	$SD_{elo}$ -SVM	$SD_{Fra}$ -SVM	Spec-SVM	VS-SVM	P-fusion-SVM
Categories	27-D	23-D	35-D	3-D	79-D	
Road	82.19	81.87	99.27	80.86	99.05	94.68
Grassland	79.19	89.49	88.41	87.82	86.31	91.57
Rubble house	87.29	64.79	80.69	61.10	88.67	88.81
Vegetation	91.75	95.19	91.68	62.60	95.40	95.12
Metal house	99.63	99.41	99.85	99.04	99.85	99.85
Bare land	76.22	74.05	80.23	70.18	84.63	80.17
Asphalt house	50.23	50.68	94.81	47.73	93.98	95.68
Brick house	82.75	85.96	92.50	80.17	95.00	96.30
Shadow	99.47	99.58	99.47	99.68	99.58	99.79
OA	81.14	84.51	87.20	79.12	90.73	93.35
Kappa	76.13	80.05	87.39	73.34	88.16	90.84

**TABLE 3:** Different Methods of Classification Accuracy Evaluation Form.

From Table3, the overall precision of the Spec-SVM classification is lower than the overall classification precision of other united spectrum-spatial characteristics, which proves that the spatial characteristics of the images can obviously improve the classification precision. The overall precisions of classifications  $SD_{spe}$ -SVM,  $SD_{elo}$ -SVM and  $SD_{Fra}$ -SVM are respectively 81.14%, 84.51% and 87.20%, if the overall classification precision of the VS-SVM model is 90.73%, the traditional VS-SVM method can improve the accuracy of classification, the extraction precision of the features, such as the asphalt houses, the roads, the brick houses, the rubble house, the bare land and so on, of which spectrums are similar to distinguish, are obviously improved. If the overall classification precisions of the feature classification model which uses the probability fusion spectrum-spatial characteristics of the support vector machines(P-fusion-SVM) are 93.35%, compared with the VS-SVM method, the precision is improved for 2.62%, and the extract precisions of the special features---the buildings are also improved: the extraction precision of the rubble house is improved for 0.14%, the precision of the metal house remains the same, the precision of the asphalt house is improved for 1.7%, and the precision of the brick house is improved for 1.3%, so it proves that the model has good classification precision, feasibility and rationality.

#### 4.2 WorldView-2 Image Experiments

We test the WorldView-2 images of Sanya, Hainan shot on January 18, 2010. The size of the experimental area is 400 rows 400 columns, the types of the features include seven classifications of the features: the roads, the shadows, the buildings, the vegetation, the water bodies, the bare land and the grassland. Figure 6 shows the data of the experimental area of the WorldView-2 images: (a) the RGB color images of the area; (b) the on-site reference data of the ground. The number of the training samples and the test samples of the images of World View-2 refers to Table 4.

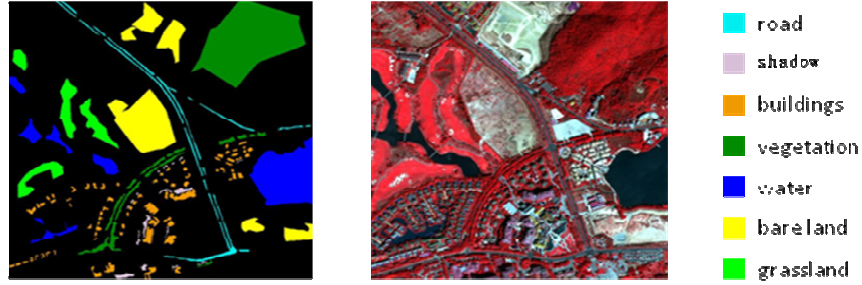


FIGURE 6: Data of the WorldView-2 Images.

Categories	Training Samples	Test Samples
Road	157	4058
Shadow	250	5655
Buildings	221	16624
Vegetation	109	1270
Water	210	25793
Bare Land	256	7435
Grass Land	102	17430

TABLE 4: Training Samples and Test Samples of the Images of WorldView-2.

Figure 7 shows the spectral curves of each classification of the features in the Sanya images, each spectral curve is responsible for a classification, and the spectral values of each classifications of the features are the mean value of the spectral reflectance of the reference samples. From the Figure, the reflectance of the two groups of the features: the buildings and the bare land, the water bodies and the shadow, is highly similar, so that the features are difficult to simply distinguish according to the spectral characteristics.

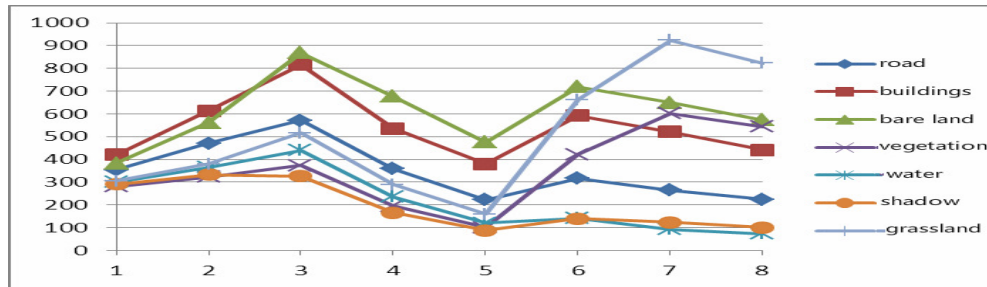
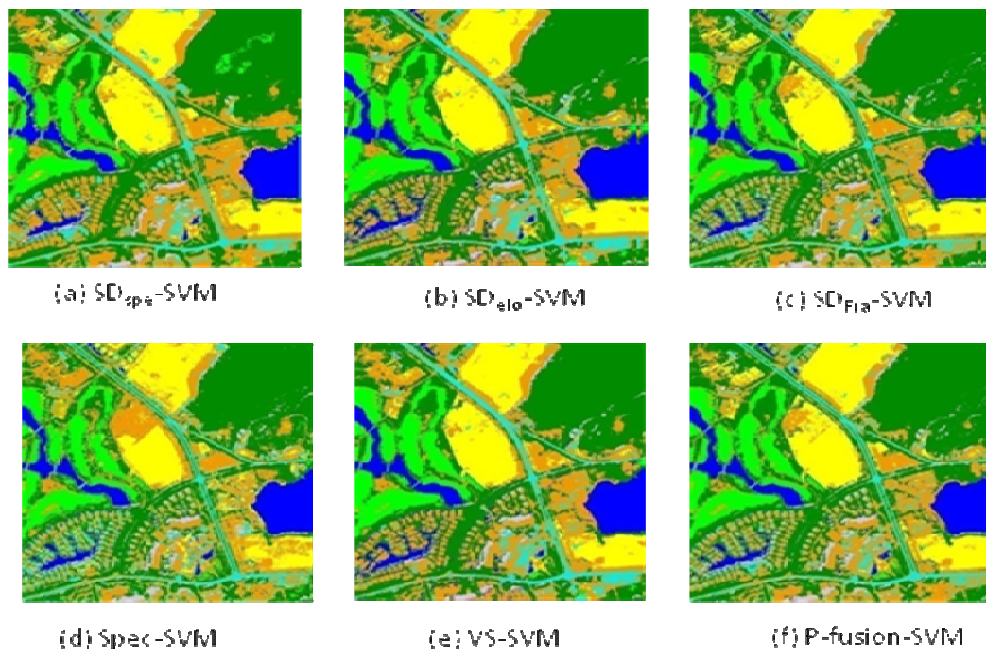


FIGURE 7: The Spectral Curves of Classifications in the Sanya Image.

Based on the description above, we apply the feature classification model of the probability fusion spectrum-spatial characteristics based on the support vector machine to this experiment. For the experiment, the specific parameters are set as follows: the number of the clusters of the spatial extension characteristics of the features  $K=20$ , the size of the window  $11 \times 11$ . The structural elements of the multi-scale morphological characteristics of the spatial extension characteristics of the features and the physical characteristics of the multi-scale morphological characteristics of the underlying surfaces of the ground, set the sizes as  $s=\{1\ 2\ 3\ 4\ 5\}$  and the directions as  $d=\{45^\circ, 90^\circ, 135^\circ, 180^\circ\}$ .

In order to compare conveniently, we introduce  $SD_{spe}\text{-SVM}$ ,  $SD_{elo}\text{-SVM}$ ,  $SD_{Fra}\text{-SVM}$ ,  $Spec\text{-SVM}$  and  $VS\text{-SVM}$  methods, and their classification results refer to Figure 8.



**FIGURE 8:** Classification Results of Sanya Image.

In order to analyze the classification of the images and the extraction results of the buildings, we evaluate the precision of the six classification methods, and the evaluation result refers to Table 5. From the Table, relative to the five methods:  $SD_{spe}$ -SVM,  $SD_{elo}$ -SVM,  $SD_{Fra}$ -SVM, Spec-SVM and VS-SVM, the overall precisions of P-fusion-SVM are respectively improved for 1.59%, 9.2%, 2.37%, 11.11% and 1.31%. The Kappa coefficients of P-SVM are respectively improved for 1.43%, 11.12%, 2.46%, 14.23% and 1.66%. The precision analysis above proves that the model improves the classification precision of the images.

Methods	$SD_{spe}$ -SVM	$SD_{elo}$ -SVM	$SD_{Fra}$ -SVM	Spec-SVM	VS-SVM	P-fusion-SVM
Categories	27-D	23-D	35-D	3-D	79-D	
road	97.81	89.33	89.60	91.01	96.80	96.16
shadow	94.72	96.22	81.89	94.88	94.41	95.43
buildings	92.93	82.94	94.27	80.58	92.60	97.50
vegetation	96.98	96.83	94.08	97.15	95.04	99.48
water	100	99.96	97.47	99.92	100	99.98
bare land	92.77	67.52	97.72	57.88	95.72	97.05
grassland	99.91	91.58	98.99	94.20	99.76	99.13
OA	96.68	89.07	95.90	87.16	96.96	98.27
Kappa	96.35	86.66	95.32	83.55	96.12	97.78

**TABLE 5:** Different Methods of Classification Accuracy Evaluation Form.

## 5. CONCLUSIONS & FUTURE WORK

The image classification model of the probability fusion spectrum-spatial characteristics based on the support vector machine uses three classifications of the spectrum-spatial characteristics ( $SD_{spe}$ -SVM,  $SD_{elo}$ -SVM,  $SD_{Fra}$ -SVM) to classify images, then carries out the

probability fusion for the classification results based on the pixels to obtain the final image classification results. For testing the feasibility of the model, we verify the model through the images of two different sensors and compare the classifications with the qualified VS-SVM model, the result shows that the model can improve the precisions of classifications.

The Classification model proposed in this paper is only aimed at the probability of a pixel fusion, does not take into account the pixel neighborhood influence on its category judgment, therefore how to reasonably consider other pixels within the scope of pixel neighborhood impact category of the classification results will be study in the future. And the various classification methods of the Classification model I proposed in this paper have the same fusion probability weighting, it may also impacts on pixel category judgment. Therefore, how to distribute the weight of each method in the model is also need further research. The Classification model proposed in this paper is combination the results of three classification methods, if there add more methods or use other methods would get better result will be study in future.

## 6. REFERENCES

- [1] Huang X., Zhang L., Li P..“An adaptive multiscale information fusion approach for feature extraction and classification of IKONOS multispectral imagery over urban areas.” *Geoscience and Remote Sensing Letters*, vol. 4, pp. 654-658, Oct. 2007.
- [2] Dell'Acqua F., Gamba P., Ferrari A., et al.“Exploiting spectral and spatial information in hyperspectral urban data with high resolution.” *Geoscience and Remote Sensing Letters*, vol. 1, pp. 322-326, Oct. 2004.
- [3] Benediktsson J. A., Palmason J. A., Sveinsson J. R..“Classification of hyperspectral data from urban areas based on extended morphological profiles.” *Geoscience and Remote Sensing*, vol. 43, pp. 480-491, Mar. 2005.
- [4] Fauvel M., Benediktsson J. A., Chanussot J., et al.“Spectral and spatial classification of hyperspectral data using SVMs and morphological profiles.” *Geoscience and Remote Sensing*, vol. 46, pp. 3804-3814, Nov. 2008.
- [5] Huang X., Zhang L..” A comparative study of spatial approaches for urban mapping using hyperspectral ROSIS images over Pavia City, northern Italy.” *International Journal of Remote Sensing*, vol. 30, pp. 3205-3221, Jun. 2009.
- [6] Waske B., Benediktsson J. A.. ”Fusion of support vector machines for classification of multisensor data.” *Geoscience and Remote Sensing*, vol. 45, pp. 3858-3866, Dec. 2007.
- [7] Pal M., Foody G. M.. “Feature selection for classification of hyperspectral data by SVM.” *Geoscience and Remote Sensing*, vol. 48, pp. 2297-2307, May 2010.
- [8] Waske B, van der Linden S, Benediktsson J A, et al. “Sensitivity of support vector machines to random feature selection in classification of hyperspectral data.” *Geoscience and Remote Sensing*, vol. 48, pp. 2880-2889, Jul. 2010.
- [9] Huang X., Zhang L..”Morphological Building/Shadow Index for Building Extraction From High-Resolution Imagery Over Urban Areas.” *Selected Topics in Applied Earth Observations and Remote Sensing*, vol. 5, pp. 161–172, Feb. 2012.
- [10] Huang X., Zhang L., Li P..”Classification and Extraction of Spatial Features in Urban Areas Using High Resolution Multispectral Imagery.” *Geoscience and Remote Sensing*, vol. 4, pp.260–264, Apr. 2007.
- [11] Ouma Y. O., Ngigi T. G., Tateishi R..”On the Optimization and Selection of Wavelet Texture for Feature Extraction from High-resolution Satellite Imagery with Application towards Urban-tree Delineation.” *International Journal of Remote Sensing*, vol. 27, pp. 73–104, Feb. 2007.

- [12] Changshan Wu, Alan T. Murray."Estimating impervious surface distribution by spectral mixture analysis." *Remote Sensing of Environment*, vol. 84, pp. 493 – 505, Apr. 2003.
- [13] Soille P., Pesaresi M.."Advances in Mathematical Morphology Applied to Geoscience and Remote Sensing." *Geoscience and Remote Sensing*, vol. 40, pp. 2042–2055, Sep. 2002.
- [14] X. Jin, Davis C. H.."Automated Building Extraction from High-resolution Satellite Imagery in Urban Areas Using Structural, Contextual, and Spectral Information" *EURASIP Journal on Applied Signal Processing*, vol. 2005, pp. 2196–2206, Jan. 2005.
- [15] Gamba P., F. Dell'Acqua, G. Lisini, and G. Trianni. "Improved VHR urban mapping exploiting feature boundaries." *Geoscience and Remote Sensing*, vol. 45, pp. 2676–2682, Aug. 2007.
- [16] Ridd, M. K."Exploring a V - I - S (vegetation - impervious surface - soil) model for urban ecosystem analysis through remote sensing: comparative anatomy for cities." *International Journal of Remote Sensing*, vol. 16, pp. 2165 – 2185, Jan. 1995.
- [17] Tian J., Chen D. M.."Optimization in Multi-scale Segmentation of High-resolution Satellite Images for Artificial Feature Recognition." *International Journal of Remote Sensing*, vol. 28, pp. 4625–4644, Sep. 2007.
- [18] Pesaresi M., Benediktsson J. A.."A New Approach for The Morphological Segmentation of High-resolution Satellite Imagery." *Geoscience and Remote Sensing*, vol. 39, pp. 309–320, Feb 2001.